

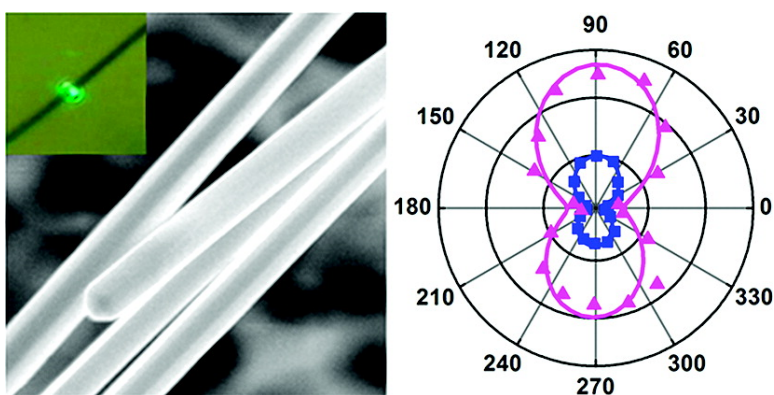
Communication

Simple Vapor-Phase Synthesis of Single-Crystalline Ag Nanowires and Single-Nanowire Surface-Enhanced Raman Scattering

Paritosh Mohanty, Ilsun Yoon, Taejoon Kang, Kwanyong Seo, Kumar S. K. Varadwaj, Wonjun Choi, Q-Han Park, Jae Pyung Ahn, Yung Doug Suh, Hyotcherl Ihee, and Bongsoo Kim

J. Am. Chem. Soc., **2007**, 129 (31), 9576-9577 • DOI: 10.1021/ja073050d • Publication Date (Web): 18 July 2007

Downloaded from <http://pubs.acs.org> on February 16, 2009



More About This Article

Additional resources and features associated with this article are available within the HTML version:

- Supporting Information
- Links to the 5 articles that cite this article, as of the time of this article download
- Access to high resolution figures
- Links to articles and content related to this article
- Copyright permission to reproduce figures and/or text from this article

[View the Full Text HTML](#)



Simple Vapor-Phase Synthesis of Single-Crystalline Ag Nanowires and Single-Nanowire Surface-Enhanced Raman Scattering

Paritosh Mohanty,[†] Ilsun Yoon,[†] Taejoon Kang,[†] Kwanyong Seo,[†] Kumar S. K. Varadwaj,[†] Wonjun Choi,[‡] Q-Han Park,[‡] Jae Pyung Ahn,[§] Yung Doug Suh,^{||} Hyotcherl Ihee,[†] and Bongsoo Kim^{*†}

Department of Chemistry, KAIST, Daejeon 305-701, Korea, Department of Physics, Korea University, Seoul 136-701, Korea, Nano-Material Research Center, KIST, Seoul 136-791, Korea, and Division of Advanced Chemical Materials, KRICT, Daejeon 305-600, Korea

Received May 1, 2007; E-mail: bongsoo@kaist.ac.kr

We report vapor-phase synthesis of single-crystalline free-standing Ag nanowires (NWs) and polarized surface-enhanced Raman scattering (SERS) of a single NW. To the best of our knowledge, vapor-phase synthesis of single-crystalline Ag NWs and polarized SERS on an individual NW have not yet been reported.

Silver has the highest electrical and thermal conductivity among all metals. In addition, because of the nature of its optical constants, silver shows the most effective SERS among all metals in the visible region.¹ Since the intensity of the SERS signal depends strongly on the detailed morphology of the Ag nanostructures, it is most important to have a well-defined and well-characterized system with a clean surface for the preparation of reliable sensors based on SERS detection. Current fabrication processes for the production of SERS-active substrates, however, are often irreproducible to a certain degree, thereby leading to inconsistent optical properties and, thus, significantly fluctuating enhancement factors for substrates prepared by apparently the same procedure. Irreproducible SERS enhancement would be detrimental to quantitative and reliable sensing, which would be most critical for medical diagnosis.

As a first step toward fabrication of well-controlled nanobiosensors employing SERS technique, we searched for a method to synthesize well-characterized free-standing single-crystalline Ag NWs with a clean surface. This led us to the adoption of vapor-phase synthesis rather than solution phase. While vapor-phase synthesis is one of the most widely used methods for the synthesis of 1D nanostructures, it has been used mainly for the synthesis of semiconductor NWs and nanotubes. Only a few metallic NWs have been synthesized through vapor phase,² and most of the reported methods for the synthesis of Ag NWs are wet chemical methods involving templates, surfactants, or capping agents.³

Our synthetic method is unique in that it uses only a single reactant, Ag₂O, without using any templates or catalysts. In a typical synthesis, 0.2 g of Ag₂O powder was placed in an alumina boat in the middle of a 1 in. diameter horizontal quartz tube furnace. The NWs were grown at a few centimeters downstream from the precursor on a Si substrate. At high temperature ($T_1 = 900\text{--}1000\text{ }^\circ\text{C}$), the precursor vapor was carried downstream by the flow of 500 sccm of Ar at 5–10 Torr to a lower temperature zone ($T_2 = 500\text{ }^\circ\text{C}$), where Ag NWs were grown. The noncatalytic growth of the NWs and the preferred formation of large particles over NWs at higher precursor temperatures demonstrated that the Ag NWs were formed by a vapor-solid mechanism.^{2a} A representative SEM image in Figure 1a shows good density of straight NWs tens of micrometers long on a Si substrate. The insets are SEM and TEM

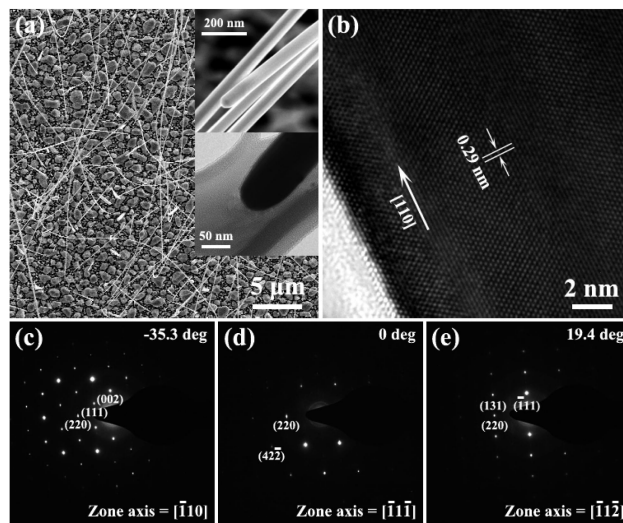


Figure 1. (a) SEM image of Ag NWs on a Si substrate. The insets are a SEM image (upper) and a TEM image (lower) of the NWs showing a round tip. (b) HRTEM image of Ag NWs. (c–e) SAED patterns of Ag NWs at various zone axes.

images of Ag NWs, showing that the tips of NWs are round, and NWs have clean surfaces and diameters of 80–150 nm.

The XRD patterns of as-grown NW ensembles (Supporting Information Figure S1) are indexed perfectly to the face-centered cubic (fcc) crystal structure of Ag ($Fm\bar{3}m$, $a = 0.4086\text{ nm}$, JCPDS 04-0783). Figure 1b shows a HRTEM image of a NW with clear lattice fringes, which reveal the single-crystalline nature of the NW. The lattice spacing is measured to be 0.29 nm, agreeing well with that of (110) planes of fcc Ag. This also shows that NWs grow along the [100] crystallographic direction. The energy-dispersive X-ray spectroscopy (EDS) mapping confirms that the NW is composed of only Ag (Figure S2). Figure 1c–e presents selected area electron diffraction (SAED) patterns of a Ag NW taken at various zone axes by rotating along the long axis of the NW. All of the spot patterns can be completely assigned to the fcc Ag structure, further confirming the single-crystallinity of the NW.

The Ag NWs prepared by solution methods have pentagonal cross-sections and are bicrystalline,⁴ whereas the free-standing NWs prepared here by vapor-phase method are single-crystalline with round cross-sections.

An optical microscope image of a single Ag NW is shown in Figure 2a. A drop of 10^{-2} M ethanolic solution of brilliant cresyl blue (BCB) was put and dried on a Si substrate. The green laser spot is seen near the center of the NW. P is a spot where the laser is focused outside the NW to obtain a SERS spectrum of the Si plate for comparison; θ is the angle between the NW axis and the

[†] KAIST.

[‡] Korea University.

[§] KIST.

^{||} KRICT.

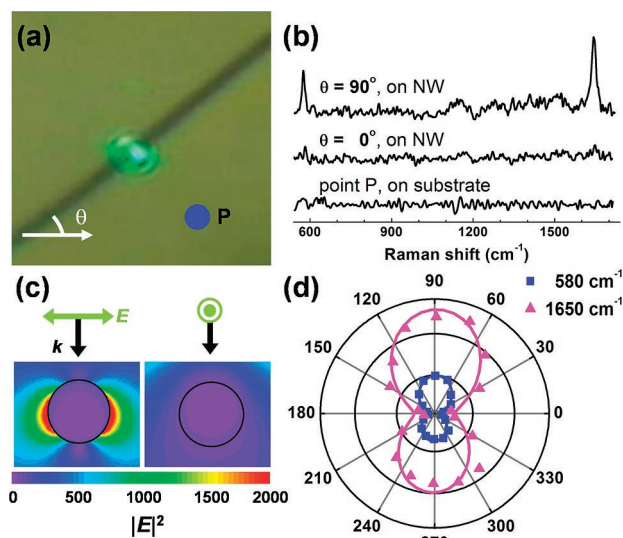


Figure 2. (a) Optical image of an individual Ag NW. The green laser spot is seen near the center of the NW. P is a spot where the laser is focused on the substrate. (b) SERS spectra of BCB adsorbed on the individual NW when $\theta = 0^\circ$ and $\theta = 90^\circ$; θ is the angle between the NW axis and the polarization of light. (c) Local electric field intensity $|E|^2$ around the NW calculated by FDTD method with different incident polarization directions. (d) Polar plots of integrated SERS intensities of the 580 and 1650 cm^{-1} Raman bands with respect to θ .

polarization of light. Figure 2b shows SERS spectra of BCB adsorbed on a single NW obtained by a homemade micro-Raman spectrometer. The top spectrum was obtained for $\theta = 90^\circ$, the middle $\theta = 0^\circ$, and the bottom at point P, respectively. The excitation wavelength was 514.5 nm, and the laser power was 0.8 mW. Strong enhancement of the SERS signal was observed when $\theta = 90^\circ$. Local electric field intensities near the NW were calculated by using the finite difference time domain (FDTD) method with the incident light of 514.5 nm (Figure 2c).⁵ Black circles represent the NWs. The diameter of the NW was set as 100 nm in the calculation. The k - and E -vectors indicate the incident direction of laser light and the polarization direction, respectively. The calculation shows that local electric field is most strongly enhanced when the NW axis is normal to the laser polarization direction, which agrees well with the observed spectra. Figure 2d shows polar plots of integrated SERS intensities of the 580 and 1650 cm^{-1} Raman bands with respect to θ . The blue and magenta lines represent best fits to a $\cos^2 \theta$ function corrected for the damping due to bleaching.⁶

To the best of our knowledge, this is the first time a SERS spectrum of a single NW is reported. Figure 2 shows that strongly anisotropic SERS enhancement can be induced by the localized excitation of a single NW, while Yang's and Moskovits's groups observed previously similar anisotropic enhancement for a mono-

layer and raft of NWs, respectively.⁷ FDTD calculation results of Figure 2c show that 514.5 nm light can excite only the transverse mode of the surface plasmon of the NW and induces strongly enhanced local electrical field near the NW.⁷

Polarization dependence of SERS has been investigated for various nanostructures, including nanoparticles, dimers and aggregates of nanoparticles, aligned NWs, and nanorod arrays.^{6–9} Whereas the classical electromagnetic field (EM) theory predicts $\cos^4 \theta$ dependence, $\cos^2 \theta$ dependence has been reported in several cases.^{7a,9c}

In summary, we showed that free-standing single-crystalline metal NWs can be synthesized in the vapor phase by an extremely simple method of using a single precursor. This new method provides NWs with a clean surface that can serve as a well-defined and well-characterized SERS-active system. We demonstrated that SERS on a single NW showed strong polarization dependence that agreed with FDTD calculation results.

Acknowledgment. This research was supported by Center for Nanostructured Materials Technology under “21st Century Frontier R&D Programs” of the MOST, Korea (06K1501-02620).

Supporting Information Available: Experimental details, including XRD, EDS, SERS results, and FDTD calculations. This material is available free of charge via the Internet at <http://pubs.acs.org>.

References

- (1) (a) Moskovits, M. *J. Raman Spectrosc.* **2005**, *36*, 485. (b) Tian, Z.-Q.; Ren, B.; Wu, D.-Y. *J. Phys. Chem. B* **2002**, *106*, 9463.
- (2) (a) Xia, Y.; Yang, P.; Sun, Y.; Wu, Y.; Mayers, B.; Gates, B.; Yin, Y.; Kim, F.; Yan, H. *Adv. Mater.* **2003**, *15*, 353. (b) Mohanty, P.; Kang, T.; Kim, B.; Park, J. *J. Phys. Chem. B* **2006**, *110*, 791.
- (3) (a) Liu, X.; Luo, J.; Zhu, J. *Nano Lett.* **2006**, *6*, 408. (b) Kline, T. R.; Tian, M.; Wang, J.; Sen, A.; Chan, M. W. H.; Mallouk, T. M. *Inorg. Chem.* **2006**, *45*, 7555. (c) Tian, M.; Wang, J.; Kurtz, J.; Mallouk, T. E.; Chan, M. H. W. *Nano Lett.* **2003**, *3*, 919. (d) Sun, Y.; Gates, B.; Mayers, B.; Xia, Y. *Nano Lett.* **2002**, *2*, 165. (e) Hu, J.-Q.; Chen, Q.; Xie, Z.-X.; Han, G.-B.; Wang, R.-H.; Ren, B.; Zhang, Y.; Yang, Z.-L.; Tian, Z.-Q. *Adv. Funct. Mater.* **2004**, *14*, 183. (f) Caswell, K. K.; Bender, C. M.; Murphy, C. J. *Nano Lett.* **2003**, 667.
- (4) (a) Sun, Y.; Mayers, B.; Herricks, T.; Xia, Y. *Nano Lett.* **2003**, *3*, 955. (b) Graff, A.; Wagner, D.; Dittbacher, H.; Kreibitz, U. *Eur. Phys. J. D* **2005**, *34*, 263.
- (5) Taflove, A.; Hagness, S. C. *Computational Electrodynamics: The Finite-Difference Time-Domain Method*, Bk&Cd ed.; Artech House: Norwood, MA, 2000.
- (6) Zhao, Y.-P.; Chaney, S. B.; Shanmukh, S.; Dluhy, R. A. *J. Phys. Chem. B* **2006**, *110*, 3153.
- (7) (a) Tao, A. R.; Yang, P. *J. Phys. Chem. B* **2005**, *109*, 15687. (b) Tao, A.; Kim, F.; Hess, C.; Goldberger, J.; He, R.; Sun, Y.; Xia, Y.; Yang, P. *Nano Lett.* **2003**, *3*, 1229. (c) Jeong, D. H.; Zhang, Y. X.; Moskovits, M. *J. Phys. Chem. B* **2004**, *108*, 12724.
- (8) (a) Wiley, B. J.; Chen, Y.; McLellan, J. M.; Xiong, Y.; Li, Z.-Y.; Ginger, D.; Xia, Y. *Nano Lett.* **2007**, *7*, 1032. (b) McLellan, J. M.; Li, Z.-Y.; Siekkinen, A. R.; Xia, Y. *Nano Lett.* **2007**, *7*, 1013.
- (9) (a) Xu, H.; Käll, M. *ChemPhysChem* **2003**, *4*, 1001. (b) Imura, K.; Okamoto, H.; Hossain, M. K.; Kitajima, M. *Nano Lett.* **2006**, *6*, 2173. (c) Brolo, A. G.; Arcatander, E.; Addison, C. J. *J. Phys. Chem. B* **2005**, *109*, 401. (d) Tian, J.-H.; Liu, B.; Li, X.; Yang, Z.-L.; Ren, B.; Wu, S.-T.; Tao, N.; Tian, Z.-Q. *J. Am. Chem. Soc.* **2006**, *128*, 14748.

JA073050D